RESEARCH ARTICLE

Microstructural alterations in the locus coeruleus-entorhinal cortex pathway in Alzheimer's disease and frontotemporal dementia

Giulia Quattrini[1,2] | **Lorenzo Pini**[3] | **Ilaria Boscolo Galazzo**[4] | **Ileana O. Jelescu**[5] | **Jorge Jovicich**[6] | **Rosa Manenti**[7] | **Giovanni B. Frisoni**[8] | **Moira Marizzoni**[1,9] | **Francesca B. Pizzini**[4] | **Michela Pievani**[1]

[1]Laboratory of Alzheimer's Neuroimaging and Epidemiology (LANE), IRCCS Istituto Centro San Giovanni di Dio Fatebenefratelli, Brescia, Italy

[2]Department of Molecular and Translational Medicine, University of Brescia, Brescia, Italy

[3]Padova Neuroscience Center, University of Padova, Padova, Italy

[4]Department of Engineering for Innovation Medicine, University of Verona, Verona, Italy

[5]Department of Radiology, Lausanne University Hospital and University of Lausanne, Lausanne, Switzerland

[6]Center of Mind/Brain Sciences, University of Trento, Rovereto, Italy

[7]Neuropsychology Unit, IRCCS Istituto Centro San Giovanni di Dio Fatebenefratelli, Brescia, Italy

[8]Memory Center and LANVIE - Laboratory of Neuroimaging of Aging, University Hospitals and University of Geneva, Geneva, Switzerland

[9]Laboratory of Biological Psychiatry, IRCCS Istituto Centro San Giovanni di Dio Fatebenefratelli, Brescia, Italy

Correspondence
Michela Pievani, PhD, Laboratory of Alzheimer's Neuroimaging and Epidemiology (LANE), IRCCS Istituto Centro San Giovanni di Dio Fatebenefratelli, via Pilastroni 4, 25125 - Brescia, Italy.
Email: mpievani@fatebenefratelli.eu

Abstract

INTRODUCTION: We investigated in vivo the microstructural integrity of the pathway connecting the locus coeruleus to the transentorhinal cortex (LC-TEC) in patients with Alzheimer's disease (AD) and frontotemporal dementia (FTD).

METHODS: Diffusion-weighted MRI scans were collected for 21 AD, 20 behavioral variants of FTD (bvFTD), and 20 controls. Fractional anisotropy (FA), mean, axial, and radial diffusivities (MD, AxD, RD) were computed in the LC-TEC pathway using a normative atlas. Atrophy was assessed using cortical thickness and correlated with microstructural measures.

RESULTS: We found (i) higher RD in AD than controls; (ii) higher MD, RD, and AxD, and lower FA in bvFTD than controls and AD; and (iii) a negative association between LC-TEC MD, RD, and AxD, and entorhinal cortex (EC) thickness in bvFTD (all $p < 0.050$).

DISCUSSION: LC-TEC microstructural alterations are more pronounced in bvFTD than AD, possibly reflecting neurodegeneration secondary to EC atrophy.

KEYWORDS
Alzheimer's disease, behavioral variant frontotemporal dementia, diffusion tensor imaging, entorhinal cortex, locus coeruleus

Highlights

- Microstructural integrity of LC-TEC pathway is understudied in AD and bvFTD.
- LC-TEC microstructural alterations are present in both AD and bvFTD.
- Greater LC-TEC microstructural alterations in bvFTD than AD.
- LC-TEC microstructural alterations in bvFTD are associated to EC neurodegeneration.

1 | INTRODUCTION

The locus coeruleus (LC) is a small brainstem nucleus located in the posterior pons, adjacent to the fourth ventricle.[1] The LC is the primary source of norepinephrine, a neurotransmitter that regulates several behavioral and cognitive processes, from arousal to memory, attention, stress, emotion, and inhibitory control.[2] The integrity of the LC, especially its rostral portion, and of its ascending noradrenergic tract has been reported to decline with age and to be associated with reduced memory performance.[3] In addition, LC dysfunction is thought to be involved in the pathophysiology of several psychiatric and neurodegenerative diseases, including Alzheimer's disease (AD) and frontotemporal dementia (FTD).[4] In AD, neuropathological studies indicate that the LC might be the earliest site of tau pathology: pre-tangle forms of tau have been observed in the LC cells before spreading to the transentorhinal (TEC; stage I), entorhinal cortex (EC; stage II), limbic, and neocortical regions (stages III-VI).[5] In FTD, LC is probably affected in a later phase than AD, as tau pathology is initially detected in the limbic cortex, including the EC (Phase I), and subsequently spreads to subcortical and brainstem nuclei (Phase II),[6] suggesting an opposite trajectory. Direct comparisons between AD and FTD indicate that LC pathological changes are generally more severe in AD,[7] possibly reflecting the different patterns of pathology spread.

Histological evidence suggests that the connectivity between the LC and the temporal cortex might be compromised in AD. Compared to controls, patients show decreased concentrations of norepinephrine in the temporal cortex and other targets of LC projections.[8] The disconnection might be related to the concomitant presence of tau pathology, which is thought to propagate along axonal pathways according to a prion-like mechanism,[9] leading to axonal injury, and cognitive impairment.[10,11] This hypothesis is supported by histological studies in AD showing that axons arising from the LC and joining to the ascending dorsal bundle of the norepinephrine system are filled with hyperphosphorylated tau.[12] Moreover, preclinical models reported that tau deposition in the LC is correlated with decreased innervation to the EC and impairment of reversal learning.[13] However, evidence of damage to this axonal pathway is mixed as other studies reported no spread of tau pathology to the EC after the injection of tau fibrils in the LC.[14,15] These results suggest that pathology might exploit connections other than axons, and their assessment *in vivo* may clarify this point. In FTD, evidence from histological and animal studies on LC axonal impairment is lacking. However, an *ex vivo* study reported higher levels of norepinephrine system in limbic regions (hippocampus and amygdala) in behavioral variant of FTD (bvFTD) than AD, while no difference was detected compared to controls.[16] A deleterious effect on LC-TEC connectivity may be hypothesized based on neuropathological evidence of pathology spread from the EC to the brainstem,[6] and of prion-like mechanisms in FTD.[9,17] Tau-related axonal injury of the LC-TEC pathway could therefore represent a key feature of AD and FTD, and the assessment of this white matter (WM) tract may provide a promising marker.

Research in context

1. **Systematic review**: We searched the literature (e.g., PubMed) for studies investigating the microstructural integrity of the locus coeruleus-transentorhinal cortex (LC-TEC) pathway in Alzheimer's disease (AD) and behavioral variant of frontotemporal dementia (bvFTD). This tract might be affected early by neurodegeneration in these diseases, however in vivo evidence of microstructural changes is very limited.

2. **Interpretation**: Our results showed that microstructural impairment of the LC-TEC pathway is detectable in both AD and bvFTD, but is more pronounced in the latter group. LC-TEC microstructural impairment was associated with entorhinal cortex atrophy in bvFTD, suggesting that these alterations might be secondary to cortical neurodegeneration.

3. **Future directions**: A deeper investigation of LC-TEC microstructural alterations in AD and related neurodegenerative diseases with diffusion imaging has the potential to clarify the pathophysiology of these disorders and to provide additional diagnostic markers.

Diffusion weighted imaging (DWI) enables to assess *in vivo* the integrity of WM axonal pathways. Diffusion tensor imaging (DTI) is the most common approach and can characterize the microstructural properties of brain tissue using four diffusivity scalar indices, that is, fractional anisotropy (FA), mean, radial, and axial diffusivities (MD, RD, and AxD, respectively).[18] To our knowledge, no neuroimaging study has yet investigated the integrity of the LC-TEC pathway in FTD. As concerns AD, only two DTI studies assessed the microstructural integrity of the LC-TEC pathway: one study found increased RD,[19] while the other one reported no change in free-water-corrected FA (i.e., FA maps after the elimination of partial volume effects of freely diffusing water).[20] These preliminary results suggested the view of LC-TEC pathway microstructural impairment in AD. However, they did not assess other measures that may provide a more comprehensive characterization of WM microstructural changes in AD, such as MD and AxD.[21]

In this study, we investigated the microstructural integrity of the LC-TEC pathway in AD and FTD using DTI. We expected to observe reduced integrity of this tract in patients compared to cognitively normal (CN) controls. Based on neuropathological evidence supporting an earlier involvement[5] and more severe LC pathological changes in AD than FTD,[7,16] we hypothesized greater LC-TEC impairment in the former group. Finally, given its anatomical connection with the EC and the role played by these regions in memory,[22] we hypothesized that LC-TEC microstructural impairment would be associated with both EC atrophy and memory deficits.

2 | METHODS

2.1 | Participants

Twenty-two AD, 22 bvFTD, and 20 CN participants were recruited in the context of the NetCogBs study (https://clinicaltrials.gov/ct2/show/NCT03422250), a clinical trial aimed at investigating imaging and cognitive longitudinal effects of a non-invasive brain stimulation protocol. Further details are provided in Supplementary materials (Appendix A). All participants provided written informed consent in accordance with the Declaration of Helsinki. The study was approved by the local Ethics Committee (Comitato Etico IRCCS San Giovanni di Dio – Fatebenefratelli, Number 43/2014).

2.2 | MRI protocol

Diffusion-weighted and structural T1-weighted MRI data were acquired on a 3T Philips Achieva system equipped with an eight-channel head coil (University Hospital of Verona, Italy). The following parameters were used: (i) for 3D T1-weighted images, TR/TE = 8/3.7 ms, flip angle = 8°, resolution = 1 mm^3 isotropic, 180 sagittal slices; (ii) for DWI (axial spin-echo EPI sequence), TR/TE = 10269/55 ms, flip angle = 90°, P > A phase-encoding, resolution = 2 mm^3 isotropic, 60 axial slices, b-value = 1000 s/mm^2; 32 directions plus 1 b = 0 s/mm^2; (iii) for 2D FLAIR, TR/TE = 9000/90 ms, TI = 2500 ms; flip angle = 150°, resolution = 0.86×0.86×5 mm^3, 35 axial slices.

2.3 | MRI processing

Diffusion-weighted data were pre-processed using the FMRIB's Diffusion Toolbox and Tract Based Spatial Statistics (TBSS), part of the FMRIB's Software Library (http://www.fmrib.ox.ac.uk/fsl/, v6.0). All 3D T1-weighted images were processed using the standard cross-sectional pipeline of FreeSurfer v6.0 (https://surfer.nmr.mgh.harvard.edu/).[23] Finally, FLAIR images were processed using the lesion prediction algorithm (LST toolbox; statistical-modelling.de/lst.html). Details on MRI data pre-processing are provided in Supplementary materials (Appendix B, Figure S1 and Figure S2).

2.4 | Statistical analysis

Statistical analyses for LC-TEC pathway DTI and morphological metrics, and for cognitive measures were performed using R (https://www.r-project.org/; version 4.0.1) and the RStudio GUI (http://www.rstudio.com/; version 1.3.1073). Non-parametric statistics was used due to the small samples and non-normal data distribution. Group differences in LC-TEC DTI, morphological, and cognitive variables were assessed using the Kruskal-Wallis test, adjusted using the Dunn-Bonferroni method for multiple comparisons. Pearson chi-square test was used for categorical variables. Significance level (p) was set to $p < 0.050$ for all tests. Associations between LC-TEC diffusion measures (FA, MD, RD, and AxD), memory (i.e., scores of immediate and delayed recall Rey Auditory Verbal Learning Test [RAVLT], Rey–Osterrieth Complex Figure [ROCF] recall, Short-Story Recall Test [SRT] recall, and Paired Associates Learning [PAL] tests), and EC thickness were assessed using the Spearman rank correlation test in AD and bvFTD separately. Only DTI measures that emerged as statistically different between CN and AD or between CN and bvFTD were considered for correlation analyses. Correlations with memory were corrected for the number of cognitive tests ($n = 5$, $p < 0.010$). Correlation slopes were compared across patients' groups using the ANOVA model and testing for interactions between slope and diagnosis. Voxelwise statistical analyses of TBSS output were performed using *randomise* (https://fsl.fmrib.ox.ac.uk/fsl/fslwiki/Randomise).[24] Skeletonized DTI maps were compared between groups using permutation-based non-parametric two-sample t-tests (number of permutations = 5000). Significance level was set to $p < 0.050$, family-wise error rate was corrected at the cluster level using the threshold-free cluster enhancement method.

Whole-brain cortical surface-based vertex-wise analyses were performed using the General Linear Model (*mri_glmfit*). Significance level was set to $p < 0.050$, cluster-wise corrected for multiple comparisons, and Bonferroni adjusted for hemispheres ($n = 2$).

3 | RESULTS

3.1 | Participants' features

Table 1 shows the demographic, clinical, and cognitive data, and the complete neuropsychological assessment of participants. Patients were more impaired than CN in all clinical features and cognitive domains (all $p < 0.050$). There were no differences between AD and bvFTD in memory scores (all $p > 0.050$), while bvFTD scored worse than AD in language, executive functions, and emotion recognition ($p < 0.050$).

3.2 | LC-TEC microstructure in AD and bvFTD

Significant differences between groups in diffusivity measures of the LC-TEC pathway are shown in Figure 1. In AD *vs.* CN, higher RD emerged in the left hemisphere ($p = 0.033$), while no differences were detected for other DTI indices (Figure 1). In bvFTD *vs.* CN, lower FA in the right LC-TEC pathway ($p = 0.018$), and higher MD, RD, and AxD bilaterally ($p < 0.006$) were detected (Figure 1).

Finally, when patient groups were compared, bvFTD revealed lower FA ($p = 0.011$), and higher MD and RD ($p = 0.030$ and $p = 0.021$, respectively) in the right LC-TEC than AD (Figure 1).

3.3 | Correlations with EC thickness

In AD, no significant association emerged between the left LC-TEC pathway microstructural impairment (i.e., increased RD) and the left EC thickness ($rho = 0.09$, $p = 0.707$).

TABLE 1 Sample features.

	CN M ± SD [range]	AD M ± SD [range]	bvFTD M ± SD [range]	Test value (df,2)	p
Demographics					
Age, years	72 ± 6 [62-83]	72 ± 6 [61-84]	70 ± 10 [52-83]	$H = 0.11$	0.944
Sex, females (%)	10 (50%)	12 (57%)	12 (60%)	$X^2 = 0.43$	0.806
Education, years	11 ± 5 [5-18]	9 ± 4 [5-18]	8 ± 4 [5-18]	$H = 5.22$	0.073
Clinical and neuropsychological assessment					
Disease duration, years	–	2 ± 2 [0-5]	2 ± 2 [0-5]	$H = 0.02$	0.882
CDR	0.0 ± 0.0 [0.0-0.0]	0.7 ± 0.2 [0.5-1.0]	0.8 ± 0.4 [0.5-2.0]	$H = 45.30$	**<0.001** *,**
MMSE	29 ± 2 [27-30]	21 ± 2 [18-25]	22 ± 4 [15-30]	$H = 36.77$	**<0.001** *,**
Vascular burden, ml	0.39 ± 0.6 [0.0-1.7]	2.6 ± 4.8 [0.1-18.6]	4.9 ± 5.0 [0.1-17.7]	$H = 20.81$	**<0.001** *,**
Memory					
RAVLT					
Immediate	46 ± 7 [33-65]	21 ± 7 [6-33]	21 ± 7 [12-39]	$H = 38.98$	**<0.001** *,**
Delayed	10 ± 2 [4-14]	1 ± 2 [0-5]	3 ± 3 [0-8]	$H = 39.95$	**<0.001** *,**
Rey–Osterrieth complex figure, recall	15 ± 4 [9-26]	2 ± 3 [0-9]	5 ± 5 [0-17]	$H = 38.55$	**<0.001** *,**
Short-Story Recall Test, total score	13 ± 3 [9-21]	3 ± 2 [0-10]	4 ± 4 [0-14]	$H = 36.62$	**<0.001** *,**
Paired Associates Learning, errors	34 ± 16 [8-64]	168 ± 27 [104-204]	145 ± 56 [22-217]	$H = 36.32$	**<0.001** *,**
Executive functions					
Trail making test					
A	46 ± 10 [26-68]	123 ± 86 [40-328]	140 ± 98 [43-443]	$H = 26.20$	**<0.001** *,**
B	129 ± 46 [60-232]	394 ± 203 [85-773]	281 ± 146 [121-531]	$H = 16.62$	**<0.001** *,**
Difference (B–A)	84 ± 45 [16-186]	312 ± 27 [42-677]	197 ± 115 [78-357]	$H = 13.96$	**<0.001** *
Digit Span					
Forward	6 ± 1 [4-7]	5 ± 1 [3-7]	4 ± 1 [3-6]	$H = 16.03$	**<0.001** **,***
Backward	4 ± 1 [0-5]	3 ± 2 [0-5]	2 ± 2 [0-5]	$H = 10.84$	**0.004** **
Visuospatial abilities					
Clock test	12 ± 1 [8-13]	6 ± 4 [0-12]	8 ± 3 [3-12]	$H = 30.77$	**<0.001** *,**
Rey–Osterrieth complex figure, copy	30 ± 4 [22-36]	21 ± 10 [0-36]	19 ± 9 [3-32]	$H = 18.61$	**<0.001** *,**
Language					
Semantic verbal fluency	40 ± 6 [29-51]	19 ± 8 [7-33]	17 ± 8 [6-36]	$H = 38.35$	**<0.001** *,**
Phonemic verbal fluency	35 ± 8 [23-52]	24 ± 10 [4-40]	13 ± 9 [1-28]	$H = 30.17$	**<0.001** *,**,***
Token test	34 ± 2 [30-37]	27 ± 5 [17-33]	24 ± 6 [12-34]	$H = 36.42$	**<0.001** *,**

(Continues)

TABLE 1   (Continued)

	CN M ± SD [range]	AD M ± SD [range]	bvFTD M ± SD [range]	Test value (df,2)	p
Emotion recognition and theory of mind					
Ekman 60-Faces Test	47 ± 5 [38-54]	40 ± 8 [23-50]	27 ± 11 [10-47]	H = 28.44	**<0.001**
Reading the mind in the eyes test	20 ± 3 [14-26]	17 ± 4 [9-25]	12 ± 4 [5-20]	H = 26.90	**<0.001** *,**

Note: Demographic, clinical, and neuropsychological assessment of 20 cognitively normal (CN) controls, 21 Alzheimer's disease (AD), and 20 behavioral variants of frontotemporal dementia (bvFTD). Values are reported as mean (M) ± standard deviation (SD) and range [min-max], or percentage (%). H and X^2 denote the Kruskall-Wallis and the Pearson's chi-squared tests' values, p denotes the significance level (set to $p < 0.050$). Significant results are reported in bold.
Abbreviations: CDR, Clinical dementia rating scare; df, degrees of freedom; MMSE, Mini-Mental State Examination; n, number; RAVLT, Rey Auditory Verbal Learning Test.
*,**,*** $p < 0.050$ for x^2 or Kruskal-Wallis test, adjusted for multiple comparisons (Dunn-Bonferroni method) for: * CN *vs* AD; ** CN *vs* bvFTD; *** AD *vs* bvFTD.
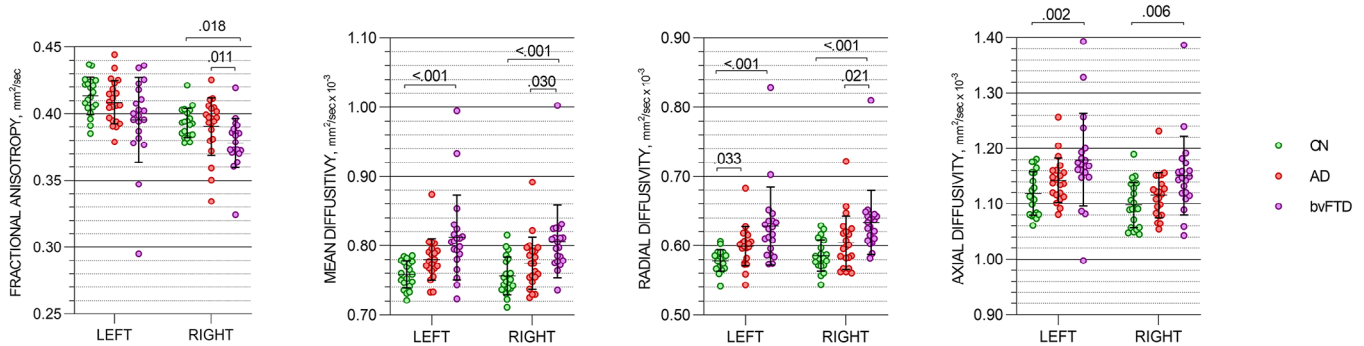
FIGURE 1   Microstructural impairment of the locus coeruleus-transentorhinal cortex (LC-TEC) pathway in AD and behavioral variant of frontotemporal dementia (bvFTD) patients. Differences between 20 cognitively normal (CN), 21 Alzheimer's disease-related dementia (AD), and 20 bvFTD patients in DTI metrics. Each dot represents a subject, horizontal and vertical bars denote the mean and the standard deviation, respectively. Values denote the statistical significance after the multiple comparisons' correction (p adjusted). Only significant results ($p < 0.050$) are reported.

In bvFTD, higher MD, higher RD, and higher AxD in the right LC-TEC pathway were negatively associated to the right EC thickness (rho = −0.68, p = 0.001; rho = −0.45, p = 0.050; rho = −0.65, p = 0.002, respectively; Figure 2). No significant results (p > 0.050) emerged when testing the correlation between the right FA and right EC thickness, nor between DTI metrics in the left hemisphere and the left EC thickness. Significant interactions between correlation slopes and diagnosis were detected for the right MD and the right RD (p < 0.015) (Figure 2).

3.4 | Correlations with memory

In AD, no significant results emerged when testing the correlation between the left RD of the LC-TEC pathway and memory (p > 0.050 for all).

In bvFTD, a negative association emerged between memory (ROCF recall score) and the right RD of LC-TEC pathway (rho = −0.46, p = 0.039), but not surviving to the multiple comparisons' corrections.

No significant results emerged when testing the correlation between the left DTI metrics and memory (p > 0.050 for all).

3.5 | Whole brain DWI and T1 analyses

The whole-brain diffusion analysis showed widespread patterns of significantly (p < 0.050) reduced FA and increased MD, RD, and AxD in patients compared to CN (Figure S3). When compared to AD, bvFTD subjects showed lower FA and higher MD, RD, and AxD in frontal and temporal tracts (Figure S3).

The regional anatomical analysis (Table S1) showed lower cortical thickness in AD and bvFTD compared to CN in bilateral temporal (including EC, hippocampus, and amygdala), frontal, and parietal lobes (p < 0.050). AD also showed lower thickness than CN in the occipital lobe (p < 0.050). Compared to bvFTD, AD showed (i) lower cortical thickness in the temporal (left fusiform gyrus), parietal (isthmus), and occipital (left lateral) cortex and, (ii) higher cortical thickness in the frontal cortex (right pars opercularis and pars orbitalis, left pars
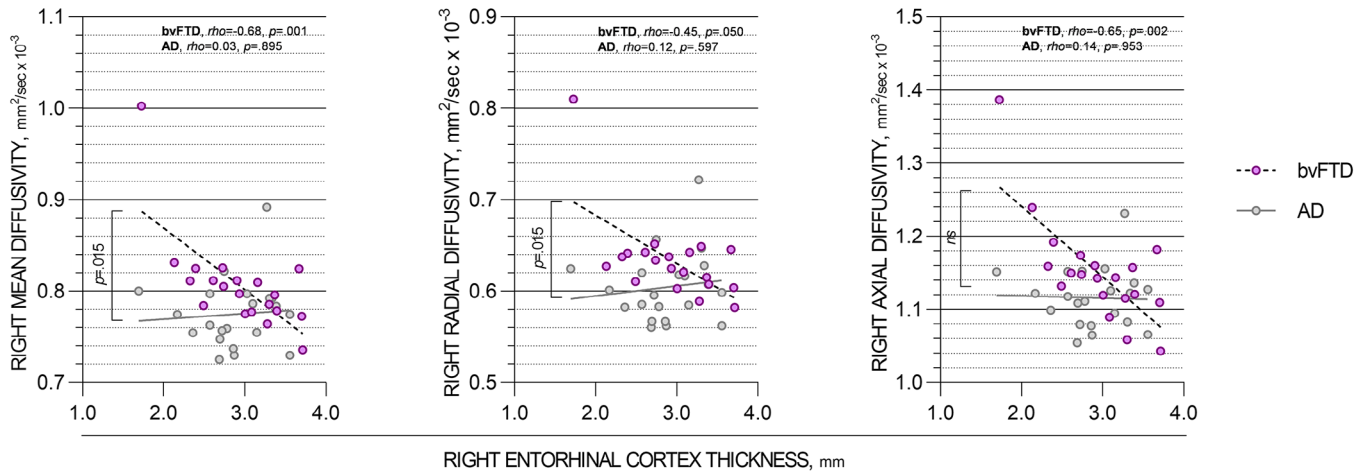
FIGURE 2 Correlations between the locus coeruleus-transentorhinal cortex (LC-TEC) microstructural changes and entorhinal cortical thickness in Alzheimer's disease (AD) and behavioral variant of frontotemporal dementia (bvFTD) patients. Significant associations were detected between diffusivity metrics of the right LC-TEC pathway and the right entorhinal cortex thickness in bvFTD. Each dot represents a subject. Rho and p values denote Spearman's rank correlation coefficient and the statistical significance (set to $p < 0.050$), respectively. Brackets denote the interaction between correlation slopes and diagnosis. ns = not significant.

triangularis, and medial orbitofrontal cortices, and bilateral orbitofrontal and frontal pole; $p < 0.050$; Table S1). Similar results were reported from the whole-brain cortical surface-based analysis (Figure S4).

4 | DISCUSSION

The assessment of the LC integrity and functioning is attracting increasing interest due to the potential of this region to provide an early biomarker for neurodegenerative diseases. Along these lines, functional and neuromelanin-sensitive imaging studies of LC have already demonstrated altered connectivity (i.e., reduced connectivity with posterior cingulate and parahippocampal cortices, increased connectivity with frontal cortex)[25] and reduced integrity[26] in AD. In contrast, evidence on LC structural connectivity is still limited in AD and completely lacking in bvFTD.

In this study, we observed significant microstructural differences in the LC-TEC pathway of bvFTD and AD relative to CN. Although whole-brain analyses revealed widespread microstructural and morphological abnormalities encompassing the temporal and EC cortex of both patient groups, LC-TEC pathway impairment predominantly emerged in bvFTD. Specifically, bvFTD showed right-lateralized reduced FA and bilaterally increased diffusivity (MD, RD, and AxD), while AD showed only left-lateralized increased RD. These MD, RD, and AxD were associated with EC thickness in bvFTD. Direct comparisons between patients confirmed that microstructural abnormalities were more pronounced in bvFTD than AD in the right LC-TEC pathway.

Our major finding is the pervasive WM degeneration of the LC-TEC pathway in bvFTD compared to CN and AD, probably reflecting the hemispheric dominance for behavioral symptoms and neurodegeneration of bvFTD.[27] To our knowledge, this is the first study showing in vivo LC-TEC microstructural impairment in bvFTD, as previous stud-

ies were almost exclusively conducted in AD or in Parkinson's disease. Our results corroborate previous neuropathological evidence pointing to an involvement of this region in FTD[6] and highlight the need of a deeper exploration and understanding of its role in this disease as well. The deterioration of WM integrity in bvFTD might reflect the deleterious effect of the underlying pathology that spreads along neuroanatomically connected brain regions.[11,28] The increased AxD and RD found in bvFTD could indicate axonal degeneration and loss, respectively.[18] Reduced FA and higher MD are traditionally also considered nonspecific sensitive markers of neurodegeneration, and they may be due to a range of degenerative phenomena (e.g., neuronal loss, fibers loss, demyelination, or a combination of them).[18] While all these mechanisms are plausible explanations for the LC-TEC pathway deterioration, the observed association between increased AxD/MD and reduced EC thickness in bvFTD is also consistent with axonal degeneration secondary to EC atrophy. While axons of the LC-TEC pathway are typically poorly myelinated[29] the presence of densely packed axon membranes is sufficient to introduce diffusion anisotropy, with much more hindered diffusion transverse than parallel to the fiber.[30] In this particular case, an increase in RD can most likely be attributed to a loss of axons, or axonal degeneration resulting in increased axonal membrane permeability. An increase in AxD could result also from increased mobility in the extra-axonal space secondary to the loss of axons or of astrocytic processes, while intra-axonal damage with changes in cytoskeleton typically result rather in decreased AxD.[31,32]

Concerning the AD group, we found a left-lateralized pattern of LC-TEC microstructural abnormalities, probably reflecting hemispheric dominance for the diseases' progression even in this case.[33] Our results were also consistent with previous DTI reports showing increased RD and no difference in FA relative to the CN.[19,20] These results are only partially in line with our hypothesis and the whole-brain diffusion analysis, as we observed only a mild impairment of this fiber notwithstanding extensive FA, MD, and AxD differences in other tracts. One possible

explanation for this unexpected result might be that our study was not sufficiently powered to detect these changes, or that the DTI metrics were not sufficiently sensitive. Still, we observed robust differences in the bvFTD group, which was comparable for size, cortical atrophy, and cognitive impairment. These results do not support the view of a direct effect of pathology on LC-TEC pathway integrity, which was hypothesized based on neuropathological data and the prion-like spread model. They are also at odds with the hypothesis of neurodegeneration secondary to EC atrophy, since we found no associations between LC-TEC microstructure metrics and EC thickness in AD, but could fit with the hypothesis of neurodegeneration secondary to LC atrophy in more advanced disease stages.[34] Of note, neuronal loss in the LC of AD has been associated with compensatory changes in the noradrenergic system such as increased release of norepinephrine.[35] Thus, we speculate that the degeneration of the LC-TEC pathway could occur only when compensatory systems fail to provide sufficient levels of this neurotransmitter. Another possible explanation may be that LC-TEC changes are masked by other concurrent processes, such as inflammation. Norepinephrine depletion has been associated with inflammation and elevated β-amyloid deposition in an AD animal model.[36] Thus, in more advanced stages of AD, reduced norepinephrine levels in the LC might be linked with neuroinflammation that negatively affect the detection of DTI alterations.[32] Neurodegeneration and inflammation have opposite effects on diffusivity measures, the former increasing diffusivity and the latter reducing it, possibly resulting in a less dramatic change in overall diffusivity when both processes are overlapping.[37,38] Furthermore, DTI dynamics over AD course are non-monotonic, in particular in relationship with amyloid burden, and cross-sectional studies suffer from the potential caveat of comparing patients at different moments on the pathological trajectory of DTI metrics.[39,40] A further possible explanation might be suggested by AD animal models, reporting that propagation might occur through alternative pathways, for example, through tracts connecting to the amygdala or olfactory cortex.[14,15]

Overall, the finding of greater LC-TEC microstructural involvement in bvFTD than AD in agreement with previous neuroimaging reports showing that WM damage is more pronounced in bvFTD,[41,42] and was also confirmed by our whole-brain diffusion analysis. These results have been previously interpreted as indicative of a greater aggressiveness in bvFTD or a different trajectory of subcortical degeneration.[41,42] Since our AD and bvFTD showed similar disease severity (Mini-Mental State Examination [MMSE] and Clinical Dementia Rating Scale [CDR] scores), disease duration, and EC neurodegeneration, both these hypotheses are plausible.

In our study, we observed a general LC-TEC microstructural asymmetry, that is, higher left than right FA values and lower left than right diffusivity values in both CN and patients. Previous DWI studies generally averaged values across hemispheres,[19,20] thus a direct comparison with our results is not feasible. However, this asymmetric pattern is consistent with previous DTI studies reporting higher left than right FA or stronger leftward connectivity in temporal regions.[43,44]

Finally, we did not observe significant associations between LC-TEC microstructural changes and memory after multiple comparisons' correction. This finding was unexpected given the close anatomical

connection of the LC-TEC with the EC and the role played by this region in memory.[22] This null result might indicate that memory deficits are more directly related to EC neurodegeneration than LC-TEC abnormalities or that our cognitive tests were not sensitive enough (e.g., due to floor effects). A *post-hoc* analysis supported the former explanation, as we observed a positive significant association between the left EC thickness and memory in both AD (RAVLT delayed, ROCF recall, and SRT scores; $rho = 0.56$, $p = 0.009$, $rho = 0.46$, $p = 0.040$, and $rho = 0.56$, $p = 0.008$, respectively) and bvFTD (PAL score; $rho = 0.48$, $p = 0.037$).

This study has several limitations that should be considered. Main limitations include the cross-sectional design and the relatively small sample size. The lack of systematic amyloid/tau biomarkers or genetic testing to confirm the clinical diagnosis in patients and to exclude early pathology in CN. Particularly, the lack of biological assessment may have limited statistical sensitivity. Biomarkers were available only for 30% of patients, thus we cannot exclude that some AD did not have amyloid pathology, nor the type of proteinopathy of FTD. Since proteinopathies differently affect gray and WM tissues,[45–48] future studies including well biologically characterized cohorts will allow for a more comprehensive assessment of LC microstructural changes in these diseases. Moreover, as we did not collect sequences sensitive to neuromelanin, we could not assess LC volumes and test whether LC-TEC microstructural changes were related to LC atrophy. Using standard atlases to derive the LC volume might overcome this limitation, but would be suboptimal at current MRI resolution, especially in a population characterized by a high degree of atrophy. Future studies with in vivo biomarkers of brain pathology and LC volumetry can properly address these issues. Finally, the sensitivity of conventional DTI metrics is probably limited in AD, and other approaches may prove more powerful. For example, Chu et al.[20] recently detected significant changes in free-water, and direct comparisons between this measure and conventional DTI metrics suggest that the former may be more sensitive to AD changes. However, free water elimination measurement requires the acquisition of at least two non-zero *b*-values to be properly determined, which is not usually available in standard DWI protocols. The sensitivity of DTI is also limited in presence of bundles with different orientations (e.g., crossing fibers), which may affect the water diffusivity. Finally, DWI collected in clinical settings often do not collect images with reverse phase encodings to correct distortions induced by susceptibility effects. Future studies using more advanced approaches (e.g., diffusion kurtosis imaging, multi-shell DWI, higher spatial resolution, two-phase encodings) might provide a better characterization of these microstructural changes.[49]

This study has also several strengths. This is the first DTI study investigating LC-TEC impairment in bvFTD and comparing these abnormalities with AD. Moreover, one advantage of DWI techniques is that they offer the possibility to assess pathology-related degeneration non-invasively, as would be the case with PET markers of amyloid and tau. This is especially relevant for the LC, as a direct assessment of tau pathology in the LC is not feasible with current PET systems resolution.

This study potentially paves the way for deeper investigations on LC assessment in neurodegenerative disease. From a clinical-diagnostic perspective, our results indicate that a conventional DTI approach (i.e., single-shell and single tensor model) might be sensitive to LC-TEC

pathway alterations in bvFTD. Finally, future studies collecting markers of tau and non-tau pathology to characterize the biological profile of patients (e.g., with cerebrospinal fluid or positron emission tomography assessment) would in vivo address the different effect proteinopathies on LC degeneration.

In conclusion, our results show that, in our patients' cohort, the microstructural impairment of the LC-TEC is greater in bvFTD than AD. These microstructural alterations might reflect neurodegeneration secondary to atrophy from the projecting region (LC in AD, EC in bvFTD). These results do not support the view of a greater microstructural LC-TEC pathway damage in AD relative to bvFTD. Future works will focus on examining the generalizability of this finding in larger clinical cohorts of AD vs bvFTD, using publicly-available data or consortia. The assessment of the LC-TEC tract may be a valuable addition to conventional DWI analysis in bvFTD to improve diagnostic classification.

AUTHORS CONTRIBUTION

ACKNOWLEDGMENTS

CONFLICT OF INTEREST STATEMENT

The authors declare that they have no competing interests. Author disclosures are available in the supporting information.

DATA AVAILABILITY STATEMENT

The data supporting the conclusions of this study can be found in Mendeley Data (doi: 10.17632/93g8gmsvnt.1).

PATIENT CONSENT STATEMENT

All participants provided written informed consent in accordance with the Declaration of Helsinki.

ORCID

Giulia Quattrini https://orcid.org/0000-0002-3750-710X
Michela Pievani https://orcid.org/0000-0002-1794-8987

REFERENCES

1. Fernandes P, Regala J, Correia F, Gonçalves-Ferreira AJ. The human locus coeruleus 3-D stereotactic anatomy. *Surg Radiol Anat.* 2012;34(10):879-885.
2. Benarroch EE. Locus coeruleus. *Cell Tissue Res.* 2018;373(1):221-232.
3. Dahl MJ, Mather M, Düzel S, et al. Rostral locus coeruleus integrity is associated with better memory performance in older adults. *Nat Hum Behav.* 2019;3(11):1203-1214.
4. Betts MJ, Kirilina E, Otaduy MC, et al. Locus coeruleus imaging as a biomarker for noradrenergic dysfunction in neurodegenerative diseases. *Brain.* 2019;142(9):2558-2571.
5. Braak H, Thal DR, Ghebremedhin E, Del Tredici K. Stages of the pathologic process in Alzheimer disease: age categories from 1 to 100 years. *J Neuropathol Exp Neurol.* 2011;70(11):960-969.
6. Irwin DJ, Brettschneider J, McMillan CT, et al. Deep clinical and neuropathological phenotyping of Pick disease. *Ann Neurol.* 2016;79(2):272-287.
7. Brunnström H, Friberg N, Lindberg E, Englund E. Differential degeneration of the locus coeruleus in dementia subtypes. *Clin Neuropathol.* 2011;30(3):104.
8. Reinikainen KJ, Paljärvi L, Huuskonen M, Soininen H, Laakso M, Riekkinen PJ. A post-mortem study of noradrenergic, serotonergic and GABAergic neurons in Alzheimer's disease. *J Neurol Sci.* 1988;84(1):101-116.
9. Wu JW, Herman M, Liu L, et al. Small misfolded Tau species are internalized via bulk endocytosis and anterogradely and retrogradely transported in neurons. *J Biol Chem.* 2013;288(3):1856-1870.
10. Digma LA, Madsen JR, Reas ET, Dale AM, Brewer JB, Banks SJ. Tau and atrophy: domain-specific relationships with cognition. *Alzheimers Res Ther.* 2019;11(1):1-12.
11. Wen Q, Risacher SL, Xie L, et al. Tau-related white-matter alterations along spatially selective pathways. *Neuroimage.* 2021;226:117560.
12. Gilvesy A, Husen E, Magloczky Z, et al. Spatiotemporal characterization of cellular tau pathology in the human locus coeruleus–pericoerulear complex by three-dimensional imaging. *Acta Neuropathol.* 2022;144(4):651-676.
13. Rorabaugh JM, Chalermpalanupap T, Botz-Zapp CA, et al. Chemogenetic locus coeruleus activation restores reversal learning in a rat model of Alzheimer's disease. *Brain.* 2017;140(11):3023-3038.
14. Ahnaou A, Rodriguez-Manrique D, Embrechts S, et al. Aging alters olfactory bulb network oscillations and connectivity: relevance for aging-related neurodegeneration studies. *Neural Plast.* 2020;2020:1703969.
15. Ahnaou A, Walsh C, Manyakov NV, Youssef SA, Drinkenburg WH. Early electrophysiological disintegration of hippocampal neural networks in a novel locus coeruleus tau-seeding mouse model of Alzheimer's disease. *Neural Plast.* 2019;2019:6981268.
16. Vermeiren Y, Janssens J, Aerts T, et al. Brain serotonergic and noradrenergic deficiencies in behavioral variant frontotemporal dementia compared to early-onset Alzheimer's disease. *J Alzheimer's Dis.* 2016;53(3):1079-1096.
17. Kim E, Hwang JL, Gaus SE, et al. Evidence of corticofugal tau spreading in patients with frontotemporal dementia. *Acta Neuropathol.* 2020;139(1):27-43.
18. Alexander AL, Lee JE, Lazar M, Field AS. Diffusion tensor imaging of the brain. *Neurotherapeutics.* 2007;4(3):316-329.
19. Sun W, Tang Y, Qiao Y, et al. A probabilistic atlas of locus coeruleus pathways to transentorhinal cortex for connectome imaging in Alzheimer's disease. *Neuroimage.* 2020;223:117301.
20. Chu WT, Wang W, Zaborszky L, et al. Association of cognitive impairment with free water in the nucleus basalis of meynert and locus coeruleus to transentorhinal cortex tract. *Neurology.* 2022;98(7):e700-e710.

21. Nir TM, Jahanshad N, Villalon-Reina JE, et al. Effectiveness of regional DTI measures in distinguishing Alzheimer's disease, MCI, and normal aging. *NeuroImage: Clinical*. 2013;3:180-195.

22. Pini L, Pievani M, Bocchetta M, et al. Brain atrophy in Alzheimer's disease and aging. *Ageing Res Rev*. 2016;30:25-48.

23. Fischl B. FreeSurfer. *Neuroimage*. 2012;62(2):774-781.

24. Winkler AM, Ridgway GR, Webster MA, Smith SM, Nichols TE. Permutation inference for the general linear model. *Neuroimage*. 2014;92:381-397.

25. Zhao S, Rangaprakash D, Venkataraman A, Liang P, Deshpande G. Investigating focal connectivity deficits in Alzheimer's disease using directional brain networks derived from resting-state fMRI. *Front Aging Neurosci*. 2017;9:211.

26. Li M, Liu S, Zhu H, et al. Decreased locus coeruleus signal associated with Alzheimer's disease based on neuromelanin-sensitive magnetic resonance imaging technique. *Front Neurosci*. 2022.

27. Gainotti G. The role of the right hemisphere in emotional and behavioral disorders of patients with frontotemporal lobar degeneration: an updated review. *Front Aging Neurosci*. 2019;11:55.

28. Kneynsberg A, Combs B, Christensen K, Morfini G, Kanaan NM. Axonal degeneration in tauopathies: disease relevance and underlying mechanisms. *Front Neurosci*. 2017;11:572.

29. Trillo L, Das D, Hsieh W, et al. Ascending monoaminergic systems alterations in Alzheimer's disease. Translating basic science into clinical care. *Neurosci Biobehav Rev*. 2013;37(8):1363-1379.

30. Beaulieu C, Allen PS. Water diffusion in the giant axon of the squid: implications for diffusion-weighted MRI of the nervous system. *Magn Reson Med*. 1994;32(5):579-583.

31. Pereira CT, Diao Y, Yin T, et al. Synchronous nonmonotonic changes in functional connectivity and white matter integrity in a rat model of sporadic Alzheimer's disease. *Neuroimage*. 2021;225:117498.

32. Winklewski PJ, Sabisz A, Naumczyk P, Jodzio K, Szurowska E, Szarmach A. Understanding the physiopathology behind axial and radial diffusivity changes—what do we know? *Front Neurol*. 2018;9:92.

33. Lubben N, Ensink E, Coetzee GA, Labrie V. The enigma and implications of brain hemispheric asymmetry in neurodegenerative diseases. *Brain Commun*. 2021;3(3):fcab211.

34. Kelly SC, He B, Perez SE, Ginsberg SD, Mufson EJ, Counts SE. Locus coeruleus cellular and molecular pathology during the progression of Alzheimer's disease. *Acta Neuropathol Commun*. 2017;5(1):1-14.

35. Szot P, White SS, Greenup JL, Leverenz JB, Peskind ER, Raskind MA. Compensatory changes in the noradrenergic nervous system in the locus ceruleus and hippocampus of postmortem subjects with Alzheimer's disease and dementia with Lewy bodies. *J Neurosci*. 2006;26(2):467-478.

36. Heneka MT, Nadrigny F, Regen T, et al. Locus ceruleus controls Alzheimer's disease pathology by modulating microglial functions through norepinephrine. *Proc Natl Acad Sci*. 2010;107(13):6058-6063.

37. Guglielmetti C, Veraart J, Roelant E, et al. Diffusion kurtosis imaging probes cortical alterations and white matter pathology following cuprizone induced demyelination and spontaneous remyelination. *Neuroimage*. 2016;125:363-377.

38. Jelescu IO, Zurek M, Winters KV, et al. In vivo quantification of demyelination and recovery using compartment-specific diffusion MRI metrics validated by electron microscopy. *Neuroimage*. 2016;132:104-114.

39. Dong JW, Jelescu IO, Ades-Aron B, et al. Diffusion MRI biomarkers of white matter microstructure vary nonmonotonically with increasing cerebral amyloid deposition. *Neurobiol Aging*. 2020;89:118-128.

40. Racine AM, Adluru N, Alexander AL, et al. Associations between white matter microstructure and amyloid burden in preclinical Alzheimer's disease: a multimodal imaging investigation. *NeuroImage: Clinical*. 2014;4:604-614.

41. Sajjadi SA, Acosta-Cabronero J, Patterson K, Diaz-de-Grenu LZ, Williams GB, Nestor PJ. Diffusion tensor magnetic resonance imaging for single subject diagnosis in neurodegenerative diseases. *Brain*. 2013;136(7):2253-2261.

42. Zhang Y, Schuff N, Du A, et al. White matter damage in frontotemporal dementia and Alzheimer's disease measured by diffusion MRI. *Brain*. 2009;132(9):2579-2592.

43. Ardekani S, Kumar A, Bartzokis G, Sinha U. Exploratory voxel-based analysis of diffusion indices and hemispheric asymmetry in normal aging. *Magn Reson Imaging*. 2007;25(2):154-167.

44. Caeyenberghs K, Leemans A. Hemispheric lateralization of topological organization in structural brain networks. *Hum Brain Mapp*. 2014;35(9):4944-4957.

45. Jiskoot LC, Bocchetta M, Nicholas JM, et al. Presymptomatic white matter integrity loss in familial frontotemporal dementia in the GENFI cohort: a cross-sectional diffusion tensor imaging study. *Ann Clin Transl Neurol*. 2018;5(9):1025-1036.

46. Chen M, Ohm DT, Phillips JS, et al. Divergent histopathological networks of frontotemporal degeneration proteinopathy subtypes. *J Neurosci*. 2022;42(18):3868-3877.

47. Josephs KA, Martin PR, Weigand SD, et al. Protein contributions to brain atrophy acceleration in Alzheimer's disease and primary age-related tauopathy. *Brain*. 2020;143(11):3463-3476.

48. Ohm DT, Peterson C, Lobrovich R, et al. Degeneration of the locus coeruleus is a common feature of tauopathies and distinct from TDP-43 proteinopathies in the frontotemporal lobar degeneration spectrum. *Acta Neuropathol*. 2020;140:675-693.

49. Jelescu IO, Budde MD. Design and validation of diffusion MRI models of white matter. *Front Phys*. 2017;5:61.

SUPPORTING INFORMATION

Additional supporting information can be found online in the Supporting Information section at the end of this article.